Int. J. Heat Mass Transfer. Vol. 34, No. 4/5, pp. 1083–1096, 1991
Printed in Great Britain

0017–9310/91 $3.00 + 0.00

Transient temperature and velocity profiles in a canned non-Newtonian liquid food during sterilization in a still-cook retort

ASHWINI KUMAR
Food Science Department, North Carolina State University, Raleigh, NC 27695-7624, U.S.A.

and

M. BHATTACHARYA
Department of Agricultural Engineering, University of Minnesota, St. Paul, MN 55108, U.S.A.

(*Received* 21 *November* 1989 *and in final form* 18 *May* 1990)

Abstract—Natural convection heating of a canned liquid food during sterilization is simulated by solving the governing equations for continuity, momentum and energy conservation for an axisymmetric case, using a finite element code. The model liquid has constant properties except viscosity (temperature dependent and shear thinning) and density (Boussinesq approximation). The velocity field establishes itself much more rapidly than the temperature field. The maximum axial velocity is of the order of 10^{-4} m s^{-1} because of low Grashof number. The coldest point is not fixed but migrates in a region that is 10–12% of the can height from the bottom of the can and at a radial distance approximately one-half of the radius. On the basis of the computed particle path it appears that the liquid initially located just below the top center is exposed to the minimum heat treatment and should be of most concern in the thermal process calculations.

INTRODUCTION

THE INVENTION of heat preserving food, by Nicholas Appert, an art as he described it in 1809, made canned food the first 'convenience' food [1]. Since then the thermal preservation of food has become more sophisticated than Appert's procedures. Conventional canning processes extend the shelf life of the food product by destroying most of the spoilage micro-organisms and also make the food safe for human consumption by destroying the pathogenic micro-organisms, mainly *Clostridium botulinum* in low-acid canned foods, present in the unprocessed food supply. A considerable amount of literature is available about the heating of food products in containers under a wide variety of conditions. Most of the mathematical analyses have been carried out for conduction-heated products because simple analytical solutions are readily available. However, detailed analysis of convection heating has usually been considered of minor importance in the food industry for two reasons: (i) high rates of transfer are often encountered in the process when agitation is used, and (ii) it is assumed that a process based on conduction heating results in a conservative design and thus can be extended to convection-heated foods as well [2]. Due to quality and economic considerations, there are instances when the product is heated primarily by natural convection in a still-retort. Examples include fruits and vegetable juices, soups, evaporated milk, broth and beer as agitation yields undesirable quality.

The time and temperature used for thermal treatment of a product in a container are based on the product characteristics, container type (glass, metal or plastic) and size, heating medium characteristics and the microbial population and its thermal inactivation kinetics. The optimum thermal process should be such that it ensures that the slowest heating point/zone (SHZ) is exposed to adequate heat treatment for sufficient time to inactivate the micro-organisms of interest [3]. The SHZ is the region of the product which receives the least sterilization during heating and cooling processes. The location of the SHZ for a convection-heated product is not as easily determined as it is for a conduction-heated product, and requires the knowledge of transient temperature and flow patterns during the sterilization process. These patterns can be found by solving the partial differential equations (mass, momentum, and energy conservation) governing the process.

Natural convection in enclosures has been studied for nuclear reactor systems, material processing, solar energy systems, energy storage and conservation, fire control, fluid and thermal sciences, and petrochemical and food industries [4]. Zechman [5] presented a survey of the experimental work involving natural convection flow patterns in food containers. Techniques such as colored dye [6, 7], particle suspension in liquids [2, 7, 8], particle streak and laser Doppler velocimetry [2] have been used to observe flow patterns inside a container. Evans *et al.* [9] measured the transient temperature profiles during natural con-

NOMENCLATURE

c_p	specific heat of liquid food [J kg^{-1} K^{-1}]
ΔE	activation energy [kJ kg mol^{-1}]
F_0	sterilization value at 121.1°C [min]
Gr	Grashof number
g	acceleration due to gravity [m s^{-2}]
H	height of the can [m]
k	thermal conductivity [W m^{-1} K^{-1}]
n	flow behavior index
p	pressure [Pa]
$\not{p}$	dimensionless pressure
Pr	Prandtl number
r	radial position from center line [m]
R	radius of the can [m]
$R(u_i)$	residual vector in equation (7)
R_g	gas constant [kJ (kg mol)$^{-1}$ K^{-1}]
R_0	reference vector in equation (7)
Ra	Rayleigh number
SHZ	slowest heating zone
t	heating time [s]
T	temperature [K]
T_w	wall temperature [K]
T_i	initial temperature [K]
u, v	velocity components in the axial and radial direction, respectively [m s^{-1}]
u, v	dimensionless axial and radial velocity components, respectively
u_i	velocity vector at the ith iteration
U	characteristic velocity [m s^{-1}]
z	axial position from bottom center of the can [m].

Greek symbols

α	thermal diffusivity [m^2 s^{-1}]
β	thermal expansion coefficient [K^{-1}]
$\dot{\gamma}$	shear rate [s^{-1}]
$\dot{\gamma}^*$	dimensionless shear rate
ε	penalty parameter
ε_{tr}	residual tolerance parameter
ε_t	local time truncation error
ε_u	velocity convergence parameter
ζ	dimensionless height, z/H
η	apparent viscosity [Pa · s]
η_0	consistency index [Pa · s^n]
η^*	dimensionless viscosity
η_{ref}	characteristic viscosity [Pa · s]
θ	dimensionless temperature
ξ	dimensionless radial position, r/R
ρ	density [kg m^{-3}]
τ	dimensionless time.

vection heating of fluid in a vertical cylinder due to uniform flux and compared their results with a simplified analytical solution. Stevens [10] tried to solve the problem numerically by solving the governing equations for natural convection heating of a liquid food in a can. His work was based on an explicit finite difference method after Torrance and Rockett [11]. Hiddink [2] also attempted a similar analysis using the finite difference methods of Barakat and Clark [12]. Both of these researchers [2, 10] had problems with their numerical schemes and were not able to resolve the solution in the bottom of the can. Engelman and Sani [13] used a finite element formulation for in-package pasteurization of beer in glass bottles and found their results in good agreement with the experimental work of Brandon *et al.* [14]. Sani [15] extended this work to the heating of beer in cans. Datta [16] used finite difference methods to solve the governing equations for sterilization of water-like food in a cylindrical can. His results were in good agreement with the experimental study of Hiddink [2].

All of the above numerical studies were carried out for water-like liquid food products having a constant viscosity. Incorporation of temperature dependence into the viscosity model makes the problem more complicated for numerical solutions. The transient temperature and velocity profiles for natural convection heating of a thick viscous liquid food (with temperature-dependent viscosity) in a cylindrical can with side heating only (the top and bottom were insulated) was presented in ref. [17]. This study was carried out for the worst case scenario where the can is placed with its bottom against the retort bottom [18] and the top was assumed to be insulated because of head space.

The numerical analysis in the present study describes sterilization of a pseudoplastic liquid food with a temperature- and shear-dependent viscosity, in a cylindrical enclosure placed in an upright position and heated on all sides in a still-retort. The specific objectives were to (i) obtain the transient temperature and velocity profiles during heating, (ii) compare simulation results with the pure conduction heating solution, (iii) study the product movement because of natural convection, and (iv) show the migration of the coldest point during heating.

PROBLEM FORMULATION

Model liquid food

Food materials are highly non-Newtonian in nature with the flow behavior index typically less than one. The viscosity model selected is given by Christiansen and Craig [19] as

$$\eta = \eta_0 \dot{\gamma}^{n-1} \exp\left(\frac{n\Delta E}{R_g T}\right). \quad (1)$$

Table 1. Properties of the liquid food used in the simulation

Property	Value[a]	Input in program
Density	950 kg m^{-3}	0.227
Specific heat (c_p)	4100 J kg^{-1} K^{-1}	79 500
Thermal conductivity (k)	0.7 W m^{-1} K^{-1}	1
Volumetric expansion coefficient (β)	0.0002 K^{-1}	1
Apparent viscosity (η)[b]:		
flow behavior index (n)	0.57	0.57
consistency index (η_0)	0.002232 Pa·s^n	0.002232 Pa·s^n
activation energy (ΔE)	30.74×10^3 kJ kg mol^{-1}	30.74×10^3 kJ kg mol^{-1}
characteristic viscosity (η_{ref})	13.57 Pa·s	13.57 Pa·s

[a] From Pereira [29].
[b] The viscosity was converted to dimensionless form in the subroutine itself.

Properties of sodium carboxy-methyl cellulose (CMC) suspended in water (0.85% w/w) was used as the model fluid for the simulation and the values for the constants used in equation (1) are given in Table 1. The shear rate is included in the model despite the usual practice of assuming that the shear rate anticipated in the natural convection heating is low (zero shear) and thus the viscosity can be assumed to behave as a Newtonian fluid [10, 17]. However, when the computed shear rate was lower than 0.01 s^{-1}, the value of η was calculated using a shear rate of 0.01 s^{-1}.

Density variations were governed by using the Boussinesq approximation which assumes that the density variation in the continuity equation can be neglected. Thus the density difference which causes the flow is approximated as a pure temperature effect, i.e. the effect of pressure on the density is neglected (incompressibility assumed). This approximation is valid for most liquids [20]. The specific heat (c_p), thermal conductivity (k) and volume expansion coefficient (β) were assumed to be constant and the values used are given in Table 1.

Description of the problem

When a container or can filled with liquid is exposed to a heating environment (still-retort), initially the liquid heats up by conduction. The rise in temperature of the liquid causes the liquid density at the wall to decrease. Due to this disparity of the liquid's density and gravity, buoyancy forces are created and lead to the movement of the liquid. Throughout the heating period, these buoyancy forces are opposed by the liquid's viscosity. The velocity of the convective current depends on the strength of the buoyancy forces and the magnitude of the resistance to flow by the liquid viscosity. This movement of liquid continues as long as the buoyancy forces are higher than viscous forces.

To simplify the problem, the following assumptions were made: (i) axisymmetry which reduces the problem from three-dimensional to two-dimensional, (ii) heat generation due to viscous dissipation is negligible, (iii) Boussinesq approximation is valid, (iv) specific heat, thermal conductivity and volume expansion coefficients are constant (Table 1), (v) the assumption of the no-slip condition at the inside wall of the can is valid, (vi) the condensing steam maintains a constant temperature at the can surface, and (vii) the thermal boundary conditions described below are applied to liquid boundaries rather than the boundaries of the can.

The specification of initial and boundary conditions for a process to be solved numerically is a critical step in obtaining a proper solution. In reality the natural convection heating of canned food is a complex process and requires time-dependent boundary conditions because of the time lag of the retort to reach the steam temperature. Initially the liquid is at rest with a uniform initial temperature of $T_i = 313$ K. To simplify the problem it is assumed that the retort reaches the desired temperature instantaneously. A common temperature used in sterilization of canned foods is 394 K. Since cans are made of metal which has a low thermal resistance and steam is condensing on the outer can wall, it can be assumed that the boundary conditions apply to the inside surface of the can (or liquid boundaries).

The governing equations were converted to dimensionless form. During natural convection, there is no free stream velocity and therefore a convection velocity, U, is employed for nondimensionalization of the velocity. This convection velocity is the maximum velocity that may be expected to occur in a natural convection process [20] and is given by $U = \sqrt{(g\beta R\Delta T)}$. The viscosity at the initial temperature (313 K) and zero shear (0.01 s^{-1}) was used as the reference viscosity (η_{ref}) for nondimensionalization. Other dimensionless variables and resulting parameters are as follows:

$$\xi = \frac{r}{R}, \quad \zeta = \frac{z}{R}, \quad \tau = \frac{tU}{R}, \quad u = \frac{u}{U}, \quad v = \frac{v}{U}$$

$$p = \frac{pR}{\eta_{ref}U}, \quad \eta^* = \frac{\eta}{\eta_{ref}}, \quad \theta = \frac{T-T_i}{T_w-T_i}, \quad \dot{\gamma}^* = \frac{R}{U}\dot{\gamma}$$

$$Ra = \frac{\rho\beta g(T_w-T_i)R^3}{\eta_{ref}\alpha}, \quad Pr = \frac{\eta_{ref}c_p}{k}.$$

With the introduction of these dimensionless variables and parameters, and the assumptions stated, the

governing equations expressing conservation of mass, momentum and energy can be expressed in the following dimensionless forms:

equation of continuity

$$\frac{1}{\xi}\frac{\partial}{\partial\xi}(\xi v)+\frac{\partial u}{\partial\zeta}=0; \tag{2}$$

equations of momentum

$$\sqrt{\left(\frac{Ra}{Pr}\right)}\left(\frac{\partial u}{\partial\tau}+v\frac{\partial u}{\partial\xi}+u\frac{\partial u}{\partial\zeta}\right)=-\frac{\partial p}{\partial\zeta}+\frac{1}{\xi}\frac{\partial}{\partial\xi}\times\left(\xi\eta^*\left(\frac{\partial u}{\partial\xi}+\frac{\partial v}{\partial\zeta}\right)\right)+2\frac{\partial}{\partial\zeta}\left(\eta^*\frac{\partial u}{\partial\zeta}\right)+\sqrt{\left(\frac{Ra}{Pr}\right)}\theta \tag{3}$$

$$\sqrt{\left(\frac{Ra}{Pr}\right)}\left(\frac{\partial v}{\partial\tau}+v\frac{\partial v}{\partial\xi}+u\frac{\partial v}{\partial\zeta}\right)=-\frac{\partial p}{\partial\xi}+\frac{\partial}{\partial\zeta}\times\left(\eta^*\left(\frac{\partial u}{\partial\xi}+\frac{\partial v}{\partial\zeta}\right)\right)+\frac{2}{\xi}\frac{\partial}{\partial\xi}\left(\xi\eta^*\frac{\partial v}{\partial\xi}\right); \tag{4}$$

equation of energy

$$\sqrt{(Ra\,Pr)}\left(\frac{\partial\theta}{\partial\tau}+v\frac{\partial\theta}{\partial\xi}+u\frac{\partial\theta}{\partial\zeta}\right)=\frac{1}{\xi}\frac{\partial}{\partial\xi}\left(\xi\frac{\partial\theta}{\partial\xi}\right)+\frac{\partial^2\theta}{\partial\zeta^2}; \tag{5}$$

and the initial condition and boundary conditions in terms of these dimensionless parameters are as follows:

$\tau = 0$ for all ξ and ζ $\qquad \theta = 0, u = 0, v = 0$

$\tau > 0$ side wall ($\xi = 1$ and $0 \leqslant \zeta \leqslant 2.74$)

$$\theta = 1, u = 0, v = 0$$

center line ($\xi = 0$ and $0 \leqslant \zeta \leqslant 2.74$)

$$\frac{\partial\theta}{\partial\xi} = 0, \frac{\partial u}{\partial\xi} = 0, v = 0$$

top surface ($0 \leqslant \xi \leqslant 1$ and $\zeta = 2.74$)

$$\theta = 1, u = 0, v = 0$$

bottom surface ($0 \leqslant \xi \leqslant 1$ and $\zeta = 0$)

$$\theta = 1, u = 0, v = 0.$$

The physical properties, temperature and velocity are thus defined by the magnitude of the equivalent dimensionless variables (Table 1). In the case of conduction heating, it was assumed that the can contained a solid with thermal diffusivity equal to that of the liquid. For this case, equation (5) was solved with the velocity terms set to zero.

Software and hardware

A commercial fluid dynamics analysis package, FIDAP (Fluid Dynamics International, Inc., Evanston, Illinois), was used to solve the governing PDEs because of its availability on the CRAY-2/4 512 Mw at the Minnesota Supercomputer Center, Minneapolis, Minnesota. This is a general purpose code that uses the finite element method (FEM). Engelman and Sani [13], Kumar *et al.* [17], Torok and Gronseth [21], Chen and Scriven [22] and others have used this code successfully to perform their simulations. A subroutine was written and linked to the FIDAP main code to calculate the viscosity from equation (1) using the computed temperature and velocity profiles.

Solution scheme

The details of the code can be found in the FIDAP manuals [23]. Various options and values of significant parameters are discussed here. FIDAP uses the penalty function approach [24] in which the continuity requirement is weakened. The value of the penalty parameter (ε) used in this simulation was 10^{-10}. The solution scheme included a fixed point iteration method (Picard iteration), variable time step increment scheme and matrix solution by direct Gauss elimination using the skyline profile method. A streamline upwinding option was used to control the velocity vector oscillation caused by advection terms in Galerkin finite element models [25]. Iteration at a given time step was terminated when the following two convergence criteria were satisfied simultaneously:

the first based on the relative error in u_i

$$\frac{\|\Delta u_i\|}{\|u_i\|} \leqslant \varepsilon_u; \quad \Delta u_i = u_i - u_{i-1} \tag{6}$$

and the second based on the residual error which must tend to zero as u_i approaches u

$$\frac{\|R(u_i)\|}{\|R_0\|} \leqslant \varepsilon_f \tag{7}$$

where $\|\cdot\|$ is an r.m.s. norm summed over all the nodes in the mesh.

The values of ε_u and ε_f used were 0.01. An additional requirement for the transient problem used was that a relative norm of the error for the next time step be less than the value of the local time truncation error (ε_t). If the norm is less than the specified ε_t then the next time increment is increased. If a transient problem is carefully monitored, the value of ε_t can be successively increased to increase the time increment and this could result in significant savings in computer time required to complete an entire simulation [26].

Temperatures and velocities are expected to have the largest variations near the wall because of the active boundary layer due to a large step increase in temperature. A non-uniform mesh (Fig. 1) with 3519 nodal points, 69 in the axial direction and 51 in the radial direction graded in both directions with a finer grid near the wall, the top and the bottom was used in the simulation. This mesh had a total of 850 nine-node isoparametric elements.

RESULTS AND DISCUSSION

CPU time and time increment history

The natural convection heating of the model liquid was simulated for 2574 s (or a dimensionless time

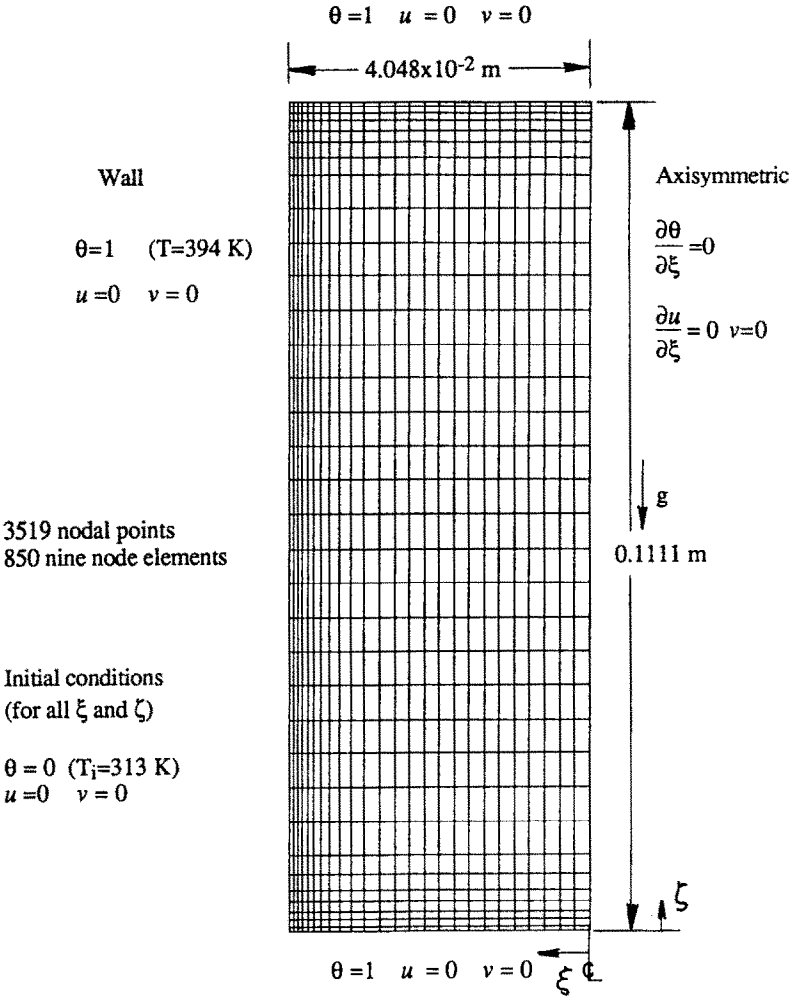

FIG. 1. Finite element mesh and boundary conditions used.

$\tau = 5096$). This required about 8 h of CPU time on the Cray-2/4 512 Mw. FIDAP is a partially vectorized code and thus could not utilize extensive vectorization capabilities of the CRAY-2. The mesh used here required about 3.5 Mw of memory which was allocated in the core itself. Preprocessing and postprocessing of the data were also carried out using FIDAP's preprocessor (FIPREP) and postprocessor (FIPOST) on the CRAY-2. Datta [16], using a finite difference formulation, reported that the problem took about 10 h of CPU time on a CDC Cyber 170/730 computer to simulate 600 s of actual heating. He used the properties of water and the viscosity was assumed constant.

The simulation history is shown in Figs. 2 and 3. As expected, more time steps with smaller values of $\Delta\tau$ were needed to resolve the flow field in the beginning (Fig. 2). It took 100 steps to achieve the first 180 s of heating, another 100 steps to reach 1000 s and 300 steps for the total of 2574 s of heating.

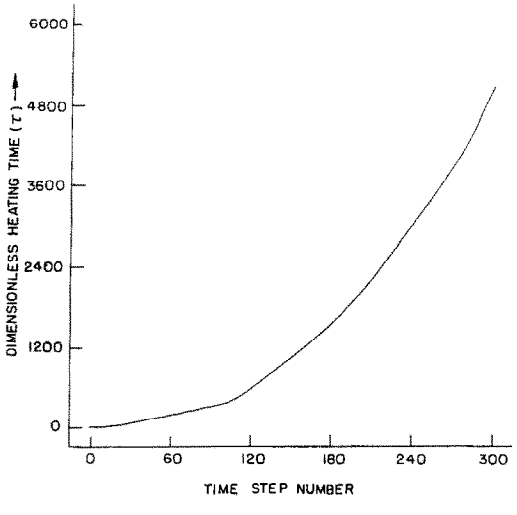

FIG. 2. Time step history: dimensionless heating time (τ) vs time step number.

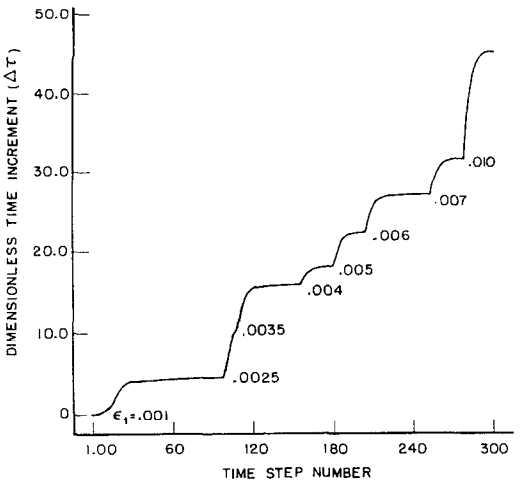

FIG. 3. Time increment history: dimensionless time increment ($\Delta\tau$) vs time step number.

As shown in Fig. 3, the value of the dimensionless time increment ranged from 0.00001 to 46.3 (5.05e − 6 to 23.4 s) and was controlled by the magnitude of the local time truncation error (ε_t). In the beginning, the velocity and the temperature fields were developing and ε_t was set to 0.001. After 100 steps ε_t was changed to 0.0025 because $\Delta\tau$ was constant at about 4.3 for the last 70 steps. It was again changed to a higher value after a few time steps (Fig. 3). Because of such a strategy, the time increment increased and the simulation was completed in a short time. Moreover this strategy did not cause any noticeable change (discontinuity or a kink) in temperature and velocity profiles. Each time step required 4–6 iterations in the beginning and 3 iterations in the latter half of the simulation.

For conduction heating, the total CPU time was about 70 s. It took 65 time steps for the entire simulation time as compared to 300 steps for the natural convection solution. The value of ε_t was 0.001 for the entire simulation. The results of the conduction heating are included for comparison purposes.

Temperature profiles

The temperature profiles during heating are presented in the form of isotherms at various times (Fig. 4), temperature histories at various points in the domain (Fig. 5) and temperatures along the center line at various times (Fig. 6). As can be seen in Fig. 4, the isotherms at $\tau = 111$ (56 s) were almost identical to pure conduction heating but with increasing time the isotherms showed a strong influence from convection currents.

This simulation did not show the presence of eddies as reported by Hiddink [2] and Datta [16] for water. The model liquid used in this simulation is more viscous ($\eta = 13.57$ Pa·s at $T = 313$ K and $\dot{\gamma} = 0.01$ s^{-1}) as compared to water ($\eta = 5.0 \times 10^{-4}$ Pa·s at $T_i = 313$ K) and thus we did not observe the formation of eddies or any recirculating zones. Hiddink [2] also did not observe a distinct eddy region in his model fluid ($\eta = 9.01$ Pa·s at 303 K and 3 Pa·s at 373 K). In the base of the can the liquid heated up by conduction first and then was swept away by the liquid moving downward and outward. The temperature profiles at nodes A, B and C in Fig. 4 confirm this assumption because the temperature increased, then decreased and then increased again.

The heating process was considerably faster for natural convection as compared to conduction only. At the end of the simulation ($\tau = 5096$), the minimum temperature for convection heating was 0.945 (389.5 K) as compared to 0.731 (372.3 K) for conduction heating (Fig. 6).

Velocity profiles

The magnitude of the velocity vector is important in natural convection studies. A few representative velocity vector plots are shown in Fig. 7 along with corresponding streamline plots. The length of the velocity vector (Fig. 7) gives the relative magnitude of the vector. The liquid at the wall was at rest because of the no-slip boundary condition. As can be seen from Fig. 4, the liquid near the wall was heated first and this lighter liquid started to move up (Fig. 7). This created a flow pattern in the domain. As this liquid reached the top, it turned toward the center core and then started moving down. The reverse of this process was true near the bottom of the can.

The velocity field developed quickly even though the temperature had not changed significantly (Figs. 4 and 7). The Prandtl number is an indication of the relative development of thermal and momentum boundary layers. A value of $Pr > 1$ means that the velocity profiles develop faster than the temperature profiles and for $Pr > 1000$, the velocity profiles develop completely before the temperature in the liquid layer has increased to any significant amount. For the liquid used in this study, the Prandtl number based on the reference viscosity (η_{ref}) was about 79 500.

As heating time increased, the temperature difference (ΔT) in the liquid also increased. This caused the buoyancy forces to increase and viscous forces to decrease (viscosity decreased with increasing temperature and shear rate). Because of this, the magnitude of the axial velocity kept increasing (Fig. 8) and peaked around $\tau = 359.6$ (180 s). By this time the buoyancy forces had started to decrease causing the reduction in the magnitude of velocity. Once the liquid approached the wall temperature the magnitude of the velocity vector was low (Fig. 7(b)).

The magnitude of the maximum axial velocity at the mid-height near the wall was about 0.31 mm s^{-1} ($\nu = 0.0038$) at $\tau = 359.6$. Hiddink [2] measured the axial velocities in a low viscosity silicone liquid ($\eta = 0.073$ Pa·s at 303 K and 0.03 Pa·s at 373 K) and in a high viscosity silicone liquid ($\eta = 9.01$ Pa·s at 303 K and 3 Pa·s at 373 K) in a container which was exposed to initial and steam temperatures of 303

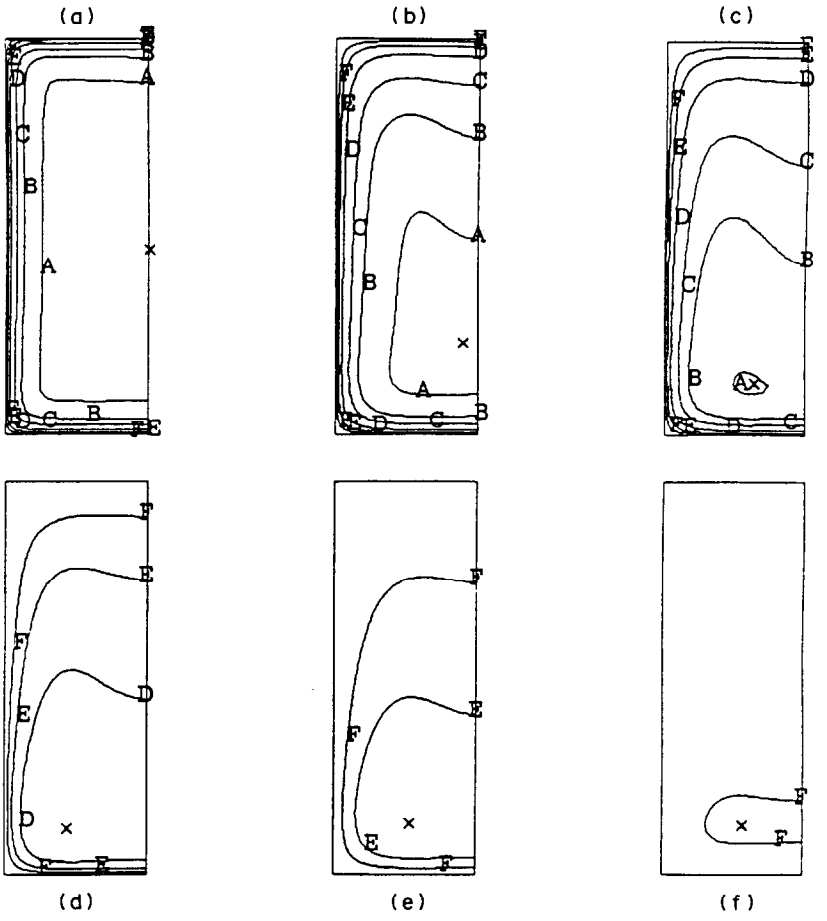

FIG. 4. Temperature contour plots for dimensionless time (τ) of (a) 119 (1 min); (b) 359.6 (3 min); (c) 619 (5 min); (d) 2389 (20 min); (e) 3520 (30 min); and (f) 5096 (42 min). Isotherms shown here are: A, $\theta = 0.0247$ (315 K); B, 0.272 (335 K); C, 0.519 (355 K); D, 0.765 (375 K); E, 0.888 (385 K); F, 0.951 (390 K). Right-hand side of each figure is center line. '×' shows the location of the coldest point in the domain.

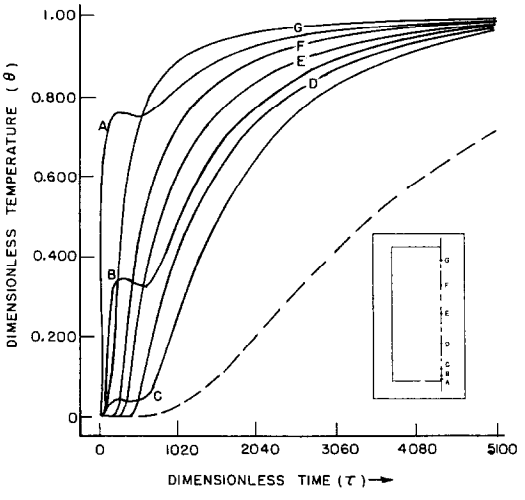

FIG. 5. Time–temperature history at various nodes on the center line. Dashed line shows the conduction time–temperature history for node at E.

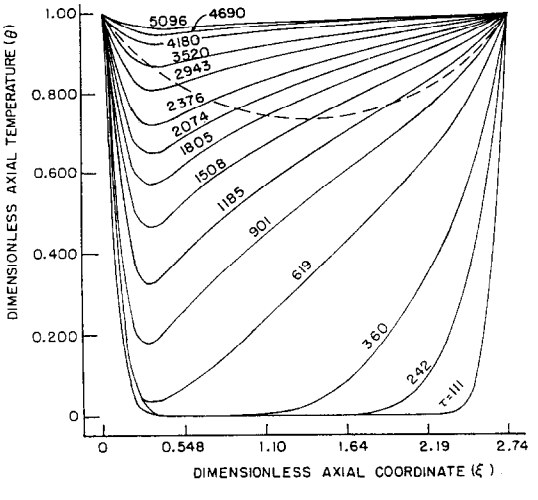

FIG. 6. Temperature along the center line for various dimensionless times. Natural convection heating. Dashed line shows the conduction data line for $\tau = 5096$.

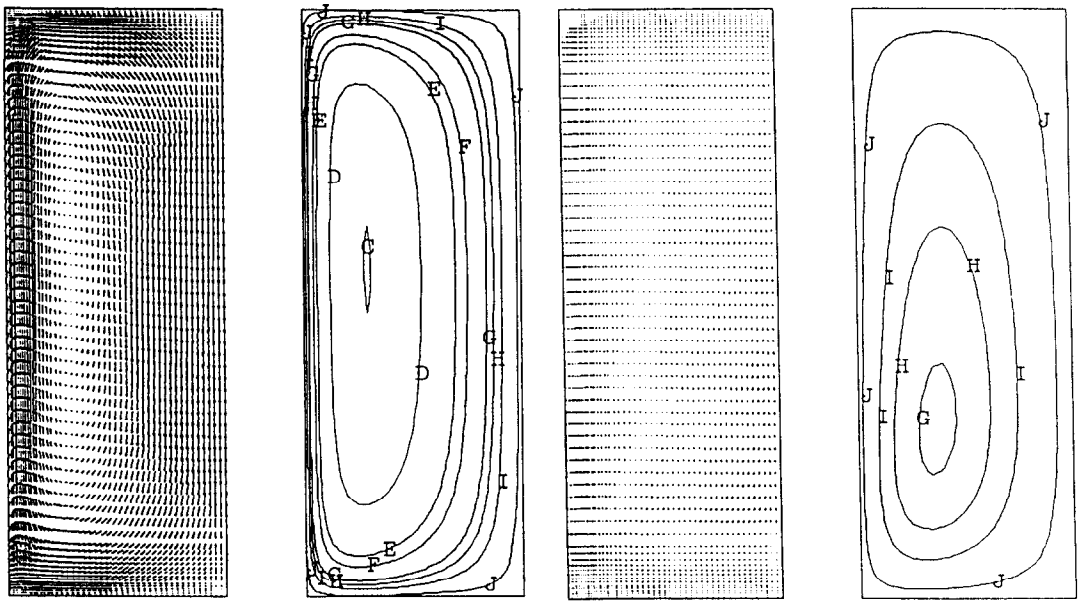

FIG. 7. Velocity vector and streamline plot at (a) $\tau = 111$ and (b) $\tau = 5096$ of dimensionless heating time. The dimensionless streamline values are: A, $-0.25e-3$; B, $-0.20e-3$; C, $-0.10e-3$; D, $-0.70e-4$; E, $-0.31e-4$; F, $-0.20e-4$; G, $-0.10e-4$; and H, $-0.10e-5$.

and 380 K, respectively. The magnitude of the velocity vector for the low viscosity fluid was about 3 mm s^{-1} after being heated for 60 s and for the high viscosity fluid it was 0.5 mm s^{-1} after 120 s of simulation. Since (i) the temperatures used in our work are higher than those of Hiddink [2], (ii) the thermal and physical properties are different, and also (iii) the viscosity is somewhere in the range of these two fluids, our results agree, qualitatively and to some extent quantitatively, with Hiddink's measurements.

Datta [16] reported that for water the maximum axial velocity was always near the wall and about 35, 16 and 12 mm s^{-1} at 30, 240 and 450 s of simulation, respectively. Because of this high velocity, the minimum temperature in the can was 357.4 K after 120 s of heating. In our case, the axial velocity at 30 s ($\tau = 59$) was in the order of 0.01 mm s^{-1} and the temperature in the domain had changed very little. The difference in the magnitude of the velocity vectors for water and the liquid used in this analysis can be explained in terms of the Grashof number, which is the ratio of the buoyancy to viscous forces and its magnitude is indicative of laminar, transition and turbulent flow regimes in natural convection flows. For viscous liquids, the viscous forces are high and thus Gr is low, e.g. for the liquid in this simulation, Gr is of the order of 0.05 (using maximum viscosity and maximum temperature difference) as compared to water where it is about 10^{10}.

Even though the velocity is changing because of increased buoyancy forces and decreased viscous forces near the wall where temperature is increasing, the maximum axial velocity was found to be in the negative direction on the center line and near the geometric center of the can for most of the time steps (Fig. 8). However, the difference between the maximum velocity near the wall and on the center line was not very large. The region of ascending liquid kept moving towards the center line (Fig. 8(b)) due to further penetration of heat in the can (Fig. 4). Hiddink [2] detected that for viscous fluid the thickness of ascending liquid region was greater than for water and attributed it to smaller axial velocities in viscous liquids. The thickness of this region was about 12–14 mm as compared to 6–7 mm for water [2, 16], 15–16 mm for a thick liquid [17], and 15–20 mm for a very viscous fluid [2].

The streamlines also provide the essential details of the flow pattern (Fig. 7). The large loops help to verify the recirculation phenomena. The absence of any smaller recirculating loops near the bottom of the can eliminates the possibility of bottom eddies. Hiddink [2], Sani [15], and Datta [16] reported the presence of these loops for water. The liquid near the bottom surface gets heated quickly and moves upward. But at the same time the core liquid is moving downward. The collision of these two fronts results in the eddies. However, in our case, it appears that the viscosity of the model fluid (higher than water) provided a cushion-effect and eliminated these secondary loops. The streamlines shifted because of the changing region of maximum activity.

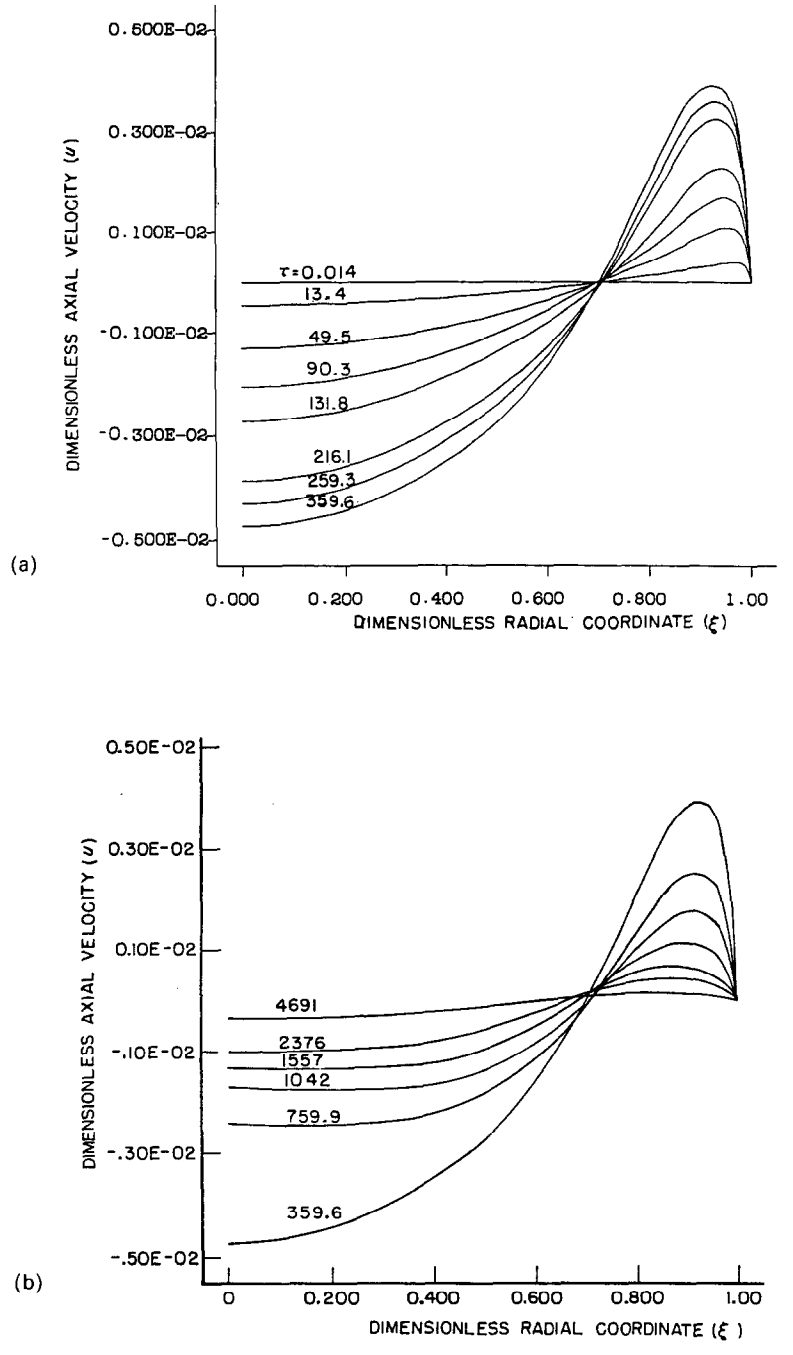

FIG. 8. Dimensionless axial velocity (u) at mid-height ($\zeta = 0.5$) vs dimensionless radial position (ξ): (a) for first $\tau = 359.6$; (b) for $\tau = 359.6$–4691.

Shear rate and temperature dependence of viscosity

The shear rate varied in the domain as a result of the changing velocity field during the simulation. Its magnitude was checked for a few time steps. At $\tau = 359.6$, it ranged from 10^{-4} to 0.24 s^{-1}. The maximum shear rate (0.24 s^{-1}) was near the wall and the minimum (10^{-4}) in the low velocity region. A value of about 0.02 s^{-1} was found near the center line. However, as mentioned earlier, a value of 0.01 s^{-1} was used to calculate the upper limit if the shear rate was less than 0.01 s^{-1}.

As mentioned earlier, all numerical simulation studies have been carried out for constant viscosity [2, 10, 13, 15, 16] or temperature-dependent viscosity [17]. The constant viscosity is derived from the viscosity at the initial temperature, retort temperature or the average of these two temperatures. Stevens [10] and Kumar *et al.* [17] also assumed the shear rate to be

very low and thus ignored the non-Newtonian aspect of the viscosity. Viscosity strongly affects the magnitude of the velocity vector. The viscosity model (equation (1)) used here has both temperature dependence and shear rate dependence terms in it. Viscosity and thus the viscous forces reduce with increase in temperature and shear rate. Since temperature is time dependent, the viscosity of the liquid goes down with time as heat penetrates the can. Keeping the buoyancy forces the same for the sake of discussion, Gr will increase. This would result in an increase in the magnitude of the velocity vectors. Similar arguments can be made for shear rate dependence of viscosity. The combined effect of the temperature and shear rate dependence would enhance the effect of natural convection on heating and thus lead to a reduction in the process time.

Movement of liquid during heating (particle path plots)

In natural convection heating the product moves as a result of density differences. This movement depends on the magnitude of the driving force, as discussed in previous sections and results in liquid displacement throughout the can. If we were to consider one fixed point in the domain (Eulerian approach, used in FIDAP), the liquid is constantly being replaced. Alternatively, if we were to track a body of liquid over simulation time (Lagrangian approach), the liquid keeps changing its position, thus being exposed to different temperatures. This requires the tracking of the moving liquid and the microbial spores being carried with it, and calculating integrated lethality in the simulation. To our knowledge, Stevens [10] is the only one who tried to incorporate the product movement in process evaluation by solving the product movement separately on the basis of the flow field; however he was not successful.

In this study the product movement is simulated from the velocity field by computing the particle path. This method is similar to an experimental procedure where a particle is introduced at various locations in the can and the movement of this particle is recorded. The numerical method assumed that a massless particle (referring to a continuous liquid material associated with a grid node) travelled on the streamline path.

To simulate movement, the particle path calculations were carried out for 18 arbitrarily chosen points of introduction (Fig. 9): six radial distances ($\xi = 0.05$, 0.2, 0.4, 0.6, 0.81 and 0.91) at three heights ($\zeta = 0.247$, 1.37 and 2.49). The path lines are not very smooth. In order to produce smooth path lines, each time step should be stored. This results in a large file for a transient simulation like the one presented here. Results from few time steps (2–5) were saved in order to limit the size of the output file and missing data were generated by interpolation. The movement of the simulated particle depended on the location of its introduction. A particle introduced at Point A at $\zeta = 0.247$ had the minimum movement because of its close proximity to the center line and to the base of the can. The particle initially at Point E at all three heights travelled the furthest. However, a particle initially at Point D at mid-height (Fig. 9) followed a

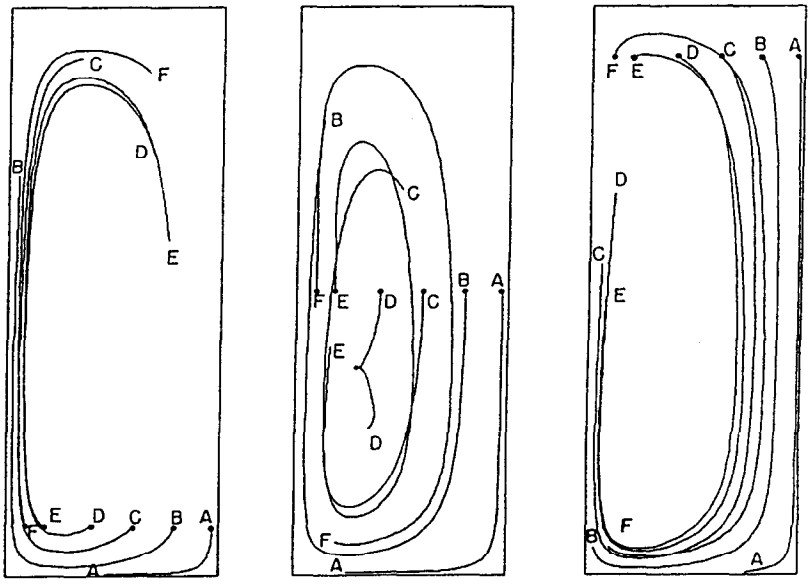

FIG. 9. Particle path plot for dimensionless heating time ($\tau = 5096$). Simulated particle injected at various points ($\xi = 0.05$, 0.2, 0.4, 0.6, 0.81 and 0.91) at three heights (a) $\zeta = 0.247$; (b) $\zeta = 1.37$; and (c) $\zeta = 2.49$ shown with '·' and distance and direction shows how far a massless particle would have travelled. Right-hand side of each figure is center line.

rather different path (particle moves down, then up and finally down again) because of the shifting streamlines as described in the previous section. The particle at this point is also travelling in the zone of least activity (Fig. 6).

If we were to calculate the lethality (microbial kill) on the basis of these particle path plots, particles introduced at different points would have accumulated different lethalities. Superposition of transient temperature profiles on the particle path and use of the Modified General Method [3] would yield a value for accumulated lethality. Qualitatively, the particles initially located at $\zeta = 2.49$ are exposed to lower temperatures and should be of most concern. All particles initially located at $\zeta = 0.247$ are exposed to high temperatures at all times because their paths are close to the can bottom and/or near the wall.

Coldest point in the can

The coldest point in the can (i.e. the location of the lowest temperature at a given time) is not a single stationary point in the liquid undergoing convection heating as is the geometric center of the can in the case of conduction-heated products. Initially the content of the can was at a uniform temperature. As heating began and the mode of heat transfer changed from conduction to convection, the coldest point moved from the geometric center to the heel of the can and towards the wall (Fig. 10). The coordinate and the process time corresponding to each letter is given in Table 2. It appears that the coldest point kept moving during heating and eventually stayed in a region that is about 10–12% of the can height from the bottom, near $\xi = 0.4$–0.6.

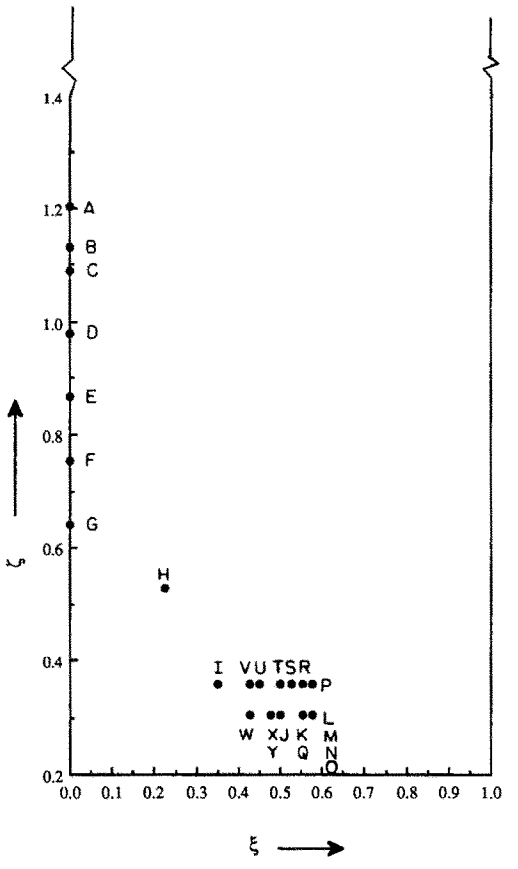

FIG. 10. Movement of the coldest point in a can during the simulation.

Traditionally, the movement of the coldest point is a critical parameter in identifying the SHZ for products in thermal process designs. The liquid and thus the bacterial spores carried with it at these locations are exposed to much less thermal treatment than the rest of the product. Also in natural convection heated products in a can being heated from all sides, the point at one-third height is considered to be the SHZ [27] and all the spores are assumed to be located at this point. Zechman and Pflug [28] reported that the SHZ is around 10% height from the bottom whereas Datta [16] found it to migrate within the bottom 15% of the can. Hiddink [2] did not observe a single point which was the coldest point in the container all the time. Based on our work and this review of the literature, it is possible that the SHZ may not be located on the vertical axis and is hard to define considering the product movement during heating. According to Zechman [5], the magnitude of the difference in the sterilization value (F_0) at the SHZ on the center line and the SHZ at some other location (if any) should be small in comparison to the overall variability that is expected in measuring F_0 of convection heated products. On the basis of the particle path plots reported here, one has to consider the movement of the liquid around the center line which may not pass through this cold point.

Once the coldest point settles in the bottom half of the container, the temperature difference between the coldest point and the center line at the same height is within ± 2 K. The usual practice of measurement of the temperature on the center line would give the temperature of the coldest point within a couple of degrees.

If there was a reduced heat transfer in the bottom of the can, i.e. temperature less than the retort temperature, because of its location in the retort, the coldest point would have moved closer to the bottom center [17]. Also it should be noted that the placement of a thermocouple in the can would disturb the symmetry of the flow pattern and possibly even move the coldest point to some other location.

SUMMARY

Sterilization of a canned liquid food in a still-retort was numerically analyzed using a finite element code (FIDAP) and the results were presented in the form of transient temperature and velocity profiles and particle path plots. Sodium carboxy-methyl cellulose was

Table 2. Information on the coldest heating point (Fig. 10)

Point (Fig. 10)	Time step number	Time, τ	Node No.	Axial distance, ζ	Radial distance, ξ	Temperature, θ
A	40	90.4	34	1.2033	0.0000	0.0000
B	50	132	32	1.1315	0.0000	0.0000
C	60	174	30	1.0908	0.0000	0.0000
D	70	216	28	0.9783	0.0000	0.0000
E	80	259	26	0.8658	0.0000	0.0000
F	90	303	24	0.7532	0.0000	0.0000
G	100	347	22	0.6407	0.0000	0.0000
H	110	446	641	0.5282	0.2258	0.0012
I	120	573	983	0.3595	0.3513	0.0012
J	132	760	1396	0.3033	0.5019	0.0064
K	141	901	1534	0.3033	0.5521	0.1250
L	150	1040	1603	0.3033	0.5772	0.1965
M	162	1240	1603	0.3033	0.5772	0.2962
N	171	1400	1603	0.3033	0.5772	0.3735
O	180	1560	1603	0.3033	0.5772	0.4448
P	192	1800	1604	0.3595	0.5772	0.5283
Q	201	2010	1534	0.3033	0.5521	0.6039
R	210	2220	1535	0.3595	0.5521	0.6629
S	222	2540	1466	0.3595	0.5270	0.7337
T	231	2780	1397	0.3595	0.5019	0.7757
U	240	3020	1259	0.3595	0.4517	0.8100
V	252	3350	1190	0.3595	0.4266	0.8462
W	261	3610	1189	0.3033	0.4266	0.8726
X	270	3890	1327	0.3033	0.4768	0.8991
Y	276	4080	1327	0.3033	0.4768	0.9136

Note: for notations, refer to Nomenclature and Fig. 10.

used as the model liquid which had temperature-dependent and shear thinning viscosity. Density variations were governed by the Boussinesq approximation. Specific heat, thermal conductivity and volume expansion coefficient were assumed to be constant.

During natural convection heating, hot liquid near the wall moved upward and cold fluid in the core moved down. The thickness of the ascending liquid near the wall was about 12–14 mm. Since the model liquid considered was viscous and gave rise to a low Grashof number, the maximum axial velocity near the wall was of the order of 10^{-4} m s^{-1}. Also there were no bottom recirculating loops or eddies formed due to bottom heating. There was no fixed point which could be called the coldest point at all times. It migrated during the initial portion of heating and eventually (after 360 s) settled in the bottom 10–12% of the height and around $\xi = 0.4$–0.6.

The movement of the liquid particles at discrete points in the domain was simulated using computed particle paths. It appears that the liquid just below the top at the beginning of heating is exposed to relatively lower temperatures during the heating and thus, this portion of liquid should be of concern in thermal process calculations.

Acknowledgements—The authors wish to acknowledge the supercomputer research grant provided by the Minnesota Supercomputer Institute, University of Minnesota; and Fluid Dynamics International, Inc., Evanston, Illinois, for its permission to use FIDAP on the Cray-2. Special thanks are due to Mr Jack Blaylock of FDI for suggestions during the simulation. This paper is published as paper No. 17626 of the Scientific Journal Series of the Minnesota Agricultural Experiment Station on research conducted under Minnesota Agricultural Experiment Station Project No. 12-030. References to commercial products and trade names made with the understanding that no discrimination and no endorsement by the University of Minnesota are implied.

REFERENCES

1. A. Lopez, *A Complete Course in Canning*. Book I. *The Canning Trade*. Baltimore, Maryland (1981).
2. J. Hiddink, Natural convection heating of liquids, with reference to sterilization of canned food, Agric. Res. Report #839, Center for Agricultural Publishing and Documentation, Wageningen, The Netherlands (1975).
3. I. J. Pflug, *A Textbook for Introductory Course in Microbiology and Engineering of Sterilization*, 6th Edn. Environmental Sterilization Lab., Minneapolis, Minnesota (1987).
4. S. Ostrach, Natural convection in enclosures, *J. Heat Transfer* **110,** 1175–1190 (1988).
5. L. G. Zechman, Natural convection heating of liquids in metal containers. Unpublished Master of Science Thesis, University of Minnesota, St. Paul, Minnesota (1983).
6. I. S. Fagerson and W. B. Esselen, Jr., Heat transfer in commercial glass containers during thermal processing, *Fd Technol.* **4,** 411–415 (1950).
7. J. L. Blaisdell, Natural convection heating of liquids undergoing sterilization in unagitated food containers, Ph.D. Dissertation, Michigan State University, East Lansing, Michigan (1963).
8. J. W. Tatom and W. O. Carlson, Transient turbulent free convection in closed containers, *Proc. Third Int. Heat Transfer Conf.*, Vol. 2, pp. 163–170 (1966).
9. L. B. Evans, R. C. Reid and E. M. Drake, Transient natural convection in a vertical cylinder, *A.I.Ch.E. Jl* **14,** 251–259 (1968).
10. P. M. Stevens, Lethality calculations, including effects of product movement, for convection heating and broken-

heating foods in still-cook retorts, Ph.D. Dissertation, University of Massachusetts, Amherst, Massachusetts (1972).
11. K. E. Torrance and J. A. Rockett, Numerical study of natural convection in an enclosure with localized heating from below: creeping flow to the onset of laminar instability, *J. Fluid Mech.* **36,** 33–54 (1969).
12. H. Z. Barakat and J. A. Clark, Analytical and experimental study of transient natural convection flows in partially filled liquid containers, *Proc. Third Int. Heat Transfer Conf.*, Vol. 2, pp. 152–162 (1966).
13. M. Engelman and R. L. Sani, Finite element simulation of an in-package pasteurization process, *Numer. Heat Transfer* **6,** 41–54 (1983).
14. H. Brandon, P. Pelton and G. Staack, State-of-the-art methodology for evaluation of pasteurizer heating and cooling processes, *MBAA Tech. Q.* **19,** 34–40 (1981).
15. R. L. Sani, Personal communication, University of Colorado, Boulder, Colorado (1987).
16. A. K. Datta, Numerical modeling of natural convection and conduction heat transfer in canned foods with application to on-line process control, Ph.D. Dissertation, University of Florida, Gainesville, Florida (1985).
17. A. Kumar, M. Bhattacharya and J. Blaylock, Numerical simulation of natural convection heating of canned thick viscous liquid food products, *J. Fd Sci.* **55,** 1403–1411 and 1420 (1990).
18. D. Naveh, I. J. Kopelman and I. J. Pflug, Sterilization of food in containers with an end flat against a retort bottom: numerical analysis and experimental measurements, *J. Fd Sci.* **49,** 1086–1093 (1984).
19. E. B. Christiansen and S. E. Craig, Heat transfer to pseudoplastic fluids in laminar flow, *A.I.Ch.E. Jl* **8,** 154–160 (1962).
20. Y. Jaluria, *Natural Convection Heat and Mass Transfer*. Pergamon Press, Oxford (1980).
21. D. Torok and R. Gronseth, Computational thermofluid applications in electronic packaging: flow and thermal fields in channels containing heating obstacles. Presented at the FIDAP User's Conf., 13–15 September 1987, Evanston, Illinois (1987).
22. K. Chen and L. E. Scriven, Three dimensional aspect of slide-die design, *Proc. 2nd FIDAP User's Conf.*, 3–4 October, Evanston, Illinois (1988).
23. M. Engelman, FIDAP, Fluid Dynamics International, Inc., Evanston, Illinois (1987).
24. M. Engelman, R. L. Sani, P. M. Gresho and M. Bercovier, Consistent vs. reduced quadrature penalty methods for incompressible media using several old and new elements, *Int. J. Numer. Meth. Fluids* **2,** 25–29 (1984).
25. A. N. Brooks and T. J. R. Hughes, Streamline upwind/Petrov–Galerkin formulations for convection dominated flows with particular emphasis on the incompressible Navier–Stokes equations, *Comp. Meth. Appl. Mech. Engng* **32,** 199–259 (1982).
26. J. Blaylock, Personal communication, Fluid Dynamics International, Inc., Evanston, Illinois (1989).
27. C. R. Stumbo, *Thermobacteriology in Food Processing*, 2nd Edn, 329pp. Academic Press, Orlando, Florida (1973).
28. L. G. Zechman and I. J. Pflug, Location of the slowest heating zone for natural convection heating fluids in metal containers, *J. Fd Sci.* **54,** 205–209, 226 (1989).
29. E. C. Pereira, Heat transfer through non-Newtonian laminar flowing fluids in a double tube heat exchanger, Ph.D. Dissertation, University of Minnesota, St. Paul, Minnesota (1988).

PROFILS VARIABLES DE TEMPERATURE ET DE VITESSE DANS UN LIQUIDE NON NEWTONIEN ENCAPSULE PENDANT LA STERILISATION

Résumé—On simule le chauffage par convection naturelle d'un liquide alimentaire dans une boite pendant la stérilisation, en résolvant les équations de continuité, de quantité de mouvement et d'énergie pour un cas axisymétrique et en utilisant un code aux éléments finis. Le liquide a des propriétés constantes sauf la viscosité (dépendant de la température et de la contrainte) et la masse volumique (approximation de Boussinesq). Le champ de vitesse s'établit plus vite que celui de température. La vitesse maximale sur l'axe est de l'ordre de 10^{-4} m s^{-1} à cause du faible nombre de Grashof. Le point le plus froid n'est pas fixe et il migre dans une région qui est de 10 à 12% de la hauteur de la boite à partir de la base et à une distance radiale égale approximativement à la moitié du rayon. Il apparait que le liquide initialement situé juste au milieu du plafond est exposé au plus faible traitement thermique et cela doit être pris en compte dans les procédés thermiques.

TRANSIENTE TEMPERATUR- UND GESCHWINDIGKEITSPROFILE IN EINEM NICHT-NEWTONSCHEN FLÜSSIGEN LEBENSMITTEL BEIM STERILISIEREN IN EINER RETORTE UNTER STILLEM SIEDEN

Zusammenfassung—Die natürliche Konvektion beim Aufheizen von einem flüssigen Lebensmittel in einem Behälter beim Sterilisieren wird unter Verwendung eines Finite-Elemente-Verfahrens durch Lösen der Erhaltungsgleichungen für Masse, Impuls und Energie bei Achsensymmetrie simuliert. Die Stoffeigenschaften der Modellflüssigkeit sind mit Ausnahme der Viskosität (Abhängigkeit von der Temperatur und Verdünnung durch Scherung) und der Dichte (Boussinesq-Approximation) konstant. Das Geschwindigkeitsfeld bildet sich sehr viel schneller aus als das Temperaturfeld. Wegen der geringen Grashof-Zahl ist die maximale axiale Geschwindigkeit von der Größenordnung 10^{-4} m s^{-1}. Der kälteste Punkt ist nicht feststehend, sondern er wandert innerhalb eines Gebietes von ungefähr 10–12% der Behälterhöhe, vom Behälterboden aus gerechnet, und in radialer Richtung innerhalb der Hälfte des Radius. Auf der Grundlage des berechneten Partikelweges scheint es, daß die Flüssigkeit, welche sich zu Beginn gerade oben in der Mitte des Behälters befand, die geringste Erwärmung erfährt. Sie sollte daher bei den wärmetechnischen Berechnungen besonders beachtet werden.

НЕСТАЦИОНАРНЫЕ ПРОФИЛИ ТЕМПЕРАТУР И СКОРОСТЕЙ В КОНСЕРВИРУЕМЫХ ПИЩЕВЫХ ПРОДУКТАХ, ПРЕДСТАВЛЯЮЩИХ СОБОЙ НЕНЬЮТОНОВСКИЕ ЖИДКОСТИ, ПРИ СТЕРИЛИЗАЦИИ В ПИЩЕВОМ ПЕРЕГОННОМ КУБЕ

Аннотация—Методом конечных элементов решены в осесимметричном случае уравнения неразрывности, сохранения количества движения и энергии для моделирования нагрева естественной конвекцией консервируемых жидких пищевых продуктов в процессе стерилизации. За исключением вязкости (зависящей от температуры и скорости сдвига) и плотности (приближение Буссинеска), модельная жидкость имеет постоянные свойства. Поле скоростей устанавливается значительно быстрей, чем температурное. Из-за низкого числа Грасгофа максимальная аксиальная скорость достигает порядка 10^{-4} м $с^{-1}$. Точка максимального охлаждения не постоянна, а перемещается в области, которая составляет 10–12% высоты контейнера (от его основания) и в радиальном направлении около половины радиуса. На основании рассчитанного пути частицы можно сделать вывод, что жидкость, первоначально находящаяся непосредственно под центральной частью верхней поверхности, в минимальной степени подвергается тепловой обработке и на нее следует обращать особое внимание при расчетах теплового процесса.